Resistance and endurance exercise training improves muscle mass and the inflammatory/fibrotic transcriptome in a rhabdomyosarcoma model

Nicolas Collao¹, Olivia Sanders¹, Taylor Caminiti¹, Laura Messeiller¹ & Michael De Lisio^{1,2}* i

¹School of Human Kinetics, University of Ottawa, Ottawa, Ontario, Canada; ²Department of Cellular and Molecular Medicine, Regenerative Medicine Program, University of Ottawa, Ottawa, Ontario, Canada

Abstract

Background Rhabdomyosarcoma (RMS) is an aggressive soft tissue sarcoma that most often develops in children. Chemoradiation therapy is a standard treatment modality; however, the detrimental long-term skeletal muscle consequences of this therapy in juvenile cancer survivors include muscle atrophy and fibrosis resulting in decreased physical performance. Using a novel model of murine resistance and endurance exercise training, we investigate its role in preventing the long-term effects of juvenile RMS plus therapy.

Methods Four-week-old male (n = 10) and female (n = 10) C57Bl/6J mice were injected with M3-9-M RMS cell into the left gastrocnemius with the right limb serving as an internal control (CON). Mice received a systemic vincristine injection and then five doses of 4.8 Gy of gamma radiation localized to the left hindlimb (RMS + Tx). Mice were then randomly divided into either sedentary (SED) or resistance and endurance exercise training (RET) groups. Changes in exercise performance, body composition, myocellular adaptations and the inflammatory/fibrotic transcriptome were assessed.

Results RET improved endurance performance (P < 0.0001) and body composition (P = 0.0004) compared to SED. RMS + Tx resulted in significantly lower muscle weight (P = 0.015) and significantly smaller myofibre cross-sectional area (CSA) (P = 0.014). Conversely, RET resulted in significantly higher muscle weight (P = 0.030) and significantly larger Type IIA (P = 0.014) and IIB (P = 0.015) fibre CSA. RMS + Tx resulted in significantly more muscle fibrosis (P = 0.028), which was not prevented by RET. RMS + Tx resulted in significantly fewer mononuclear cells (P < 0.05) and muscle satellite (stem) cells (MuSCs) (P < 0.05) and significantly more immune cells (P < 0.05) than CON. RET resulted in significantly more fibro-adipogenic progenitors (P < 0.05), a trend for more MuSCs (P = 0.076) than SED and significantly more endothelial cells specifically in the RMS + Tx limb. Transcriptomic changes revealed significantly higher expression of inflammatory and fibrotic genes in RMS + Tx, which was prevented by RET. In the RMS + Tx model, RET also significantly altered expression of genes involved in extracellular matrix turnover.

Conclusions Our study suggests that RET preserves muscle mass and performance in a model of juvenile RMS survivorship while partially restoring cellular dynamics and the inflammatory and fibrotic transcriptome.

Keywords cachexia; cancer; chemotherapy; exercise; fibro-adipogenic progenitors; fibrosis; inflammation; muscle satellite cells; radiation

Received: 22 June 2022; Revised: 14 December 2022; Accepted: 16 January 2023
*Correspondence to: Michael De Lisio, School of Human Kinetics, University of Ottawa, Ottawa, ON, Canada. Email: mdelisio@uottawa.ca
Nicolas Collao and Olivia Sanders contributed equally to this work.

Introduction

Rhabdomyosarcoma (RMS) is an intramuscular cancer and is the most common juvenile soft tissue sarcoma.¹ Although survival is as high as 90%, themoradiation therapy used to treat RMS causes muscle atrophy and fibrosis in 80% survivors.² As a result, juvenile sarcoma survivors experience a high prevalence of muscle weakness, fatigue, exercise intolerance and disability.3 A reduction in muscle satellite (stem) cells (MuSCs), 4,5 increased expression of fibrotic genes and inflammation have been implicated as mechanisms responsible for these late effects in skeletal muscle. 6 MuSCs, quiescent myogenic cells, are located in the periphery of the muscle fibre between the sarcolemma and the basal lamin⁷ and are required for pre-pubertal skeletal muscle growth.8 Proper MuSC regulation requires a functioning niche consisting of vascular endothelial cells (ECs), immune cells and fibro-adipogenic progenitors (FAPs), among other cell types.9 Cancer therapy is known to deplete ECs in several tissues 10 and alters immune cell phenotype and function in skeletal muscle, which contributes to impaired muscle regeneration. 11 The effects of cancer therapy on FAPs have received relatively less attention; however, early evidence suggests that cancer therapy does not impact FAP content in mice.⁶ As such, interventions to prevent deleterious alterations to niche-mediated MuSC dysfunction in juvenile cancer survivors may improve long-term outcomes.

Resistance and endurance exercise training (RET) is recommended for cancer survivors as an effective non-pharmacological strategy to improve muscle strength, endurance performance and quality of life in cancer survivors. These recommendations are derived primarily from adult survivors of breast, prostate and colorectal cancer with no specific recommendations for juvenile cancer survivors. Mechanistically, endurance exercise training reduces radiation-induced oxidative stress in skeletal muscle and increases MuSC and FAP content in post-pubertal mice. Methanistical muscle late effects in a preclinical model of juvenile RMS plus therapy survival remains unknown.

To begin to elucidate the mechanisms responsible for RET-induced improvements in skeletal muscle in cancer survivors, we combine these newly established models of juvenile RMS plus therapy,⁵ and progressive RET,¹⁶ to examine the extent to which RET improves skeletal muscle quality and quantity. We hypothesized that RET would prevent several of the skeletal muscle defects induced by juvenile RMS plus therapy by improving cellular components and gene expression of soluble factors in the MuSC niche.

Methods

Experimental design

Ethical approval for this project was obtained from the University of Ottawa Animal Care and Veterinary Service Committee and performed according to the Canadian Council on Animal Care's guidelines. Mice were housed specific pathogen-free conditions in a controlled facility (temperature $22-25^{\circ}$ C, 30% humidity and 12-h light: dark cycle), and food and water were provided ad libitum. Four-week-old male (n=10) and female (n=10) C57Bl/6 mice (Jackson Laboratory) acclimatized to the animal facility for 1 week prior to use in any experiments.

The RMS + Tx model was conducted as previously described (*Figure 1A*).⁵ All mice were injected with 100 000 M3-9-M cells in sterile phosphate-buffered saline (PBS) into the left gastrocnemius (RMS + Tx).¹⁷ The contralateral right gastrocnemius was injected with sterile PBS as an internal control (CON). Mice recovered for 3 days and then received an intraperitoneal injection of vincristine sulfate (1 mg/kg, Cat# V8388, Sigma-Aldrich). At 5 weeks of age, all mice were exposed to fractioned radiation of five doses of 4.8 Gy (X-RAD 320, Precision X-Ray Irradiation) localized to the RMS-injected (left) limb (RMS + Tx). The rest of the body was protected using a lead murine abdomen shield, and the contralateral non-RMS-injected, non-irradiated (right) limb was used as an internal control (CON).

At 6 weeks of age, mice were randomly assigned into either a RET or sedentary (SED) group. Mice in the RET group were individually housed with weighted running wheels, whereas mice in the SED group were housed with no wheel for 8 weeks. 16 After 1 week of wheel acclimatization with no weight, RET began with a 2 g resistance in Week 1, which progressed by 1 g/week until a weight of 5 g was maintained for 2 weeks (Weeks 4 and 5) and then increased to 6 g, which was maintained for the final 3 weeks (Weeks 6-8) as previously described. 16 Running distance (km/day) was tracked using low-profile wireless running wheels (ENV-044 and ENV-047, Med Associates) and associated software packages (Wheel Manager Software SOF-860, Med Associates). The design resulted in four groups with the within factors (i.e., contralateral limbs of the same mouse) of CON and RMS + Tx and the between factors (i.e., independent mice) of SED and RET: (1) CON-SED, (2) CON-EX, (3) RMS + Tx-SED and (4) RMS + Tx-RET. Animals were euthanized 4 days after the final exercise session with CO2 asphyxiation followed by cervical dislocation. The left (RMS + Tx) and right (CON) gastrocnemius were resected, weighed and partitioned into thirds for downstream analyses.

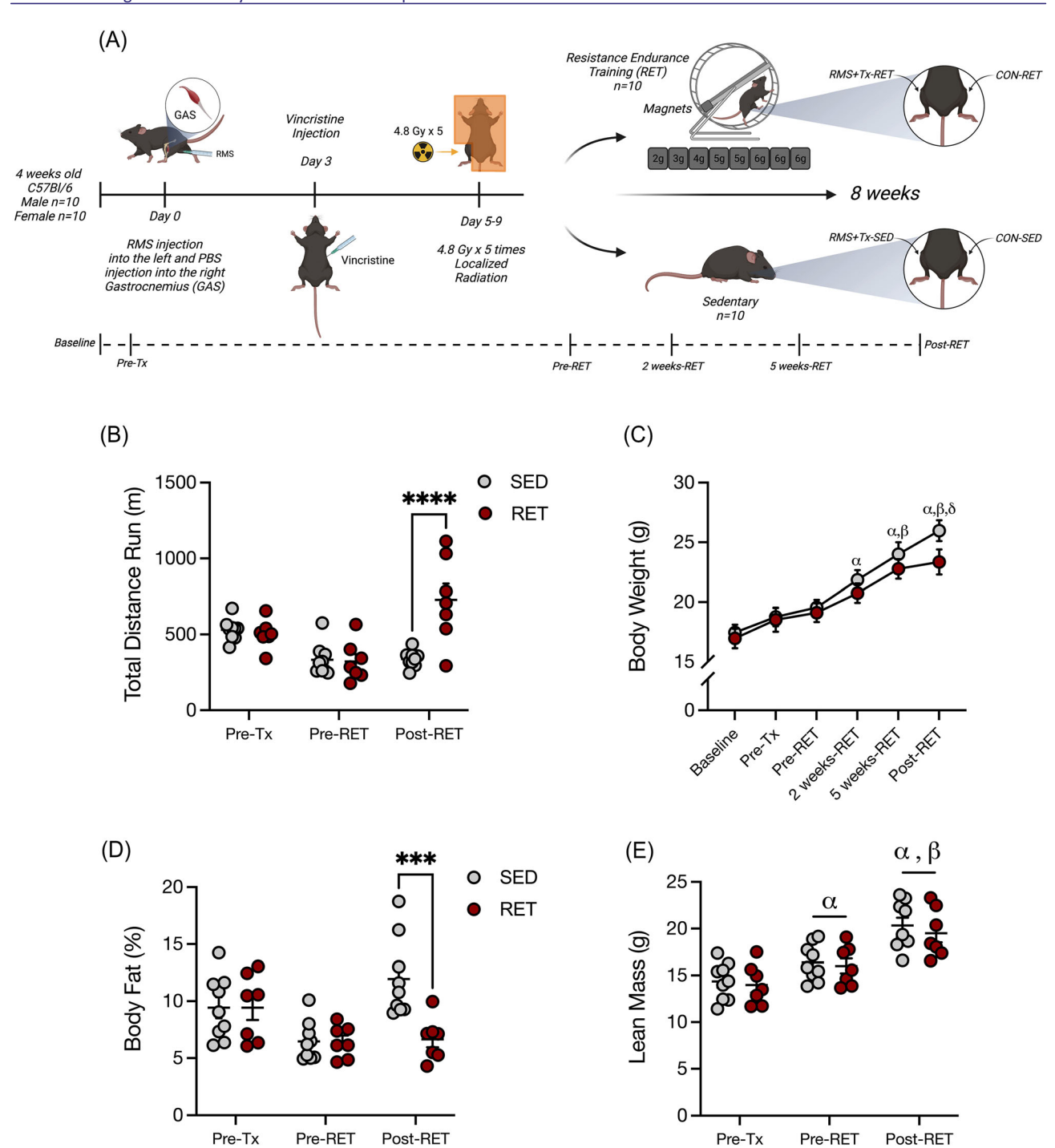


Figure 1 Resistance and endurance exercise training (RET) improves endurance performance, body composition and muscle weight following rhabdomyosarcoma (RMS) plus therapy. (A) Study design. Four-week-old male (n = 10) and female (n = 10) C57Bl/6 mice received M3-9-M RMS cell injections into the left gastrocnemius to generate the tumours with the left limb serving injected with phosphate-buffered saline (PBS) as an internal control (CON). After 3 days, all mice received systemic vincristine treatment administered by intraperitoneal (i.p.) injection. Two days after chemotherapy, mice were administered with five doses of 4.8 Gy of gamma radiation localized to the left hindlimb only (RMS + Tx). Following treatment, mice were randomly divided into either sedentary (SED) or resistance and endurance exercise training (RET) groups for 8 weeks. Figure created with Biorender. com. (B) Endurance performance assessed by total distance run (m) until volitional exhaustion. (C) Body weight (g). (D) Body fat percentage and (E) lean mass (g). ****P < 0.001 and *****P < 0.0001, SED versus RET. In (C), $\alpha = \text{significantly}$ different than baseline, Pre-Tx and Pre-RET; $\beta = \text{significantly}$ different than 2-week RET; and $\sigma = \text{significantly}$ different than Pre-RET. Three-way analysis of variance (ANOVA) or two-way ANOVA (E), Sidak post hoc test. n = 7-9 per group.

Rabdomyosarcoma cell line

M3-9-M RMS cells (gift from Mackall Lab, Stanford) were cultured in RPMI media 1640 (Cat# 350-000-CL, Wisent Inc) containing 1% L-glutamine (Cat# 07100, STEMCELL Technologies), 10% heat-inactivated foetal bovine serum (Cat# 12483-020, Gibco), HEPES (Cat# 15630-080, Gibco), 1% non-essential amino acids (Cat# 11140-050, Gibco), 1% sodium pyruvate (Cat# 11360-070, Gibco), 1% penicillin/streptomycin (P/S) (Cat# 15140-122, Thermo Fisher Scientific) and 50 mM 2-mercaptoethanol (Cat# 21985-023, Gibco). 17

Body composition and performance testing

Body composition and body weight were assessed by EchoMRI-900 (EchoMRI LLC) and an electronic scale as previously described. 18,19 Endurance performance was evaluated on a motorized treadmill as previously described without electric shock. 19 Testing ceased when mice met one of the following three criteria to end the test: (1) resisted stimulation with rubberized tweezers, (2) remained stationary on the treadmill platform off of the belt for > 2 min or (3) remained one body length away from the platform for > 5 s and could not increase speed when stimulated. 19 Maximal grip strength of forelimbs and hindlimbs combined was measured as previously described¹⁹ using a Chatillon DFE II (Columbus Instruments). A total of five grip strength tests were performed on each mouse with each mouse grasping the force grid with all four limbs. The highest and lowest force values were discarded, and an average of the remaining three values were used to score each mouse. Body composition and performance tests were conducted before treatment (Pre-Tx), before RET (Pre-RET) and after RET (Post-RET).

Histochemical, immunostaining and microscopy

The distal third of the gastrocnemius was then embedded in tissue-embedding medium (OCT, Cat# 4585, Fisher Scientific) prior to freezing in liquid nitrogen-cooled isopentane (Cat# 277258-1L, Sigma-Aldrich); 10-μm transverse sections were collected using a HM 525 NX-2210 cryostat (Leica, Wetzlar, Germany) and placed onto glass slides (Cat# 12-544-2, Fisher Scientific). An average of 482 ± 22.5 myofibres per mouse were analysed for cross-sectional area (CSA), fibre-type proportion and myonuclear domain. Masson's trichrome^{15,20} and myosin heavy chain (MyHC)²¹ staining and analysis were conducted as previously described. The following isotype-specific anti-mouse primary antibodies were used: MyHC-I, IgG-2b (1:100, Cat# BA-D5, DSHB), MyHC-IIA, IgG1 (1:100, Cat# SC-71, DSHB), MyHC-IIB, IgM (1:25, Cat# BF-F3, DSHB), and anti-laminin, IgG (1:50, Cat# MA1-06100 Monoclonal Antibody (A5), Thermo Fisher Scientific) with their corresponding secondary antibodies: Alexa Fluor® 647 AffiniPure Goat Anti-Mouse IgG, Fcy subclass 2b specific (1:100, Cat# 115-605-207, Cedarlane Laboratories), Alexa Fluor® 488 AffiniPure Goat Anti-Mouse IgG, Fcy subclass 1 specific (1:100, Cat# 115-545-205, Cedarlane Laboratories), Cy[™]3 AffiniPure Fab Fragment Goat Anti-Mouse IgM, μ chain specific (1:50, Cat# 115-167-020, Cedarlane Laboratories), and Alexa Fluor 594 (Cat# A11005, Invitrogen). Type IIx fibres were identified as unstained for MyHC-I, MyHC-IIA or MyHC-IIB. Hybrid fibres were identified as those staining for > 1 MyHC isoform. Myonuclei were identified as nuclei with at least 50% of their area beneath the basal lamina. Myonuclear domain was calculated by dividing the number of myonuclei by the CSA (µm²) per fibre. Images for Masson's trichrome staining were acquired using an EVOS-FL2 Automated Microscope (Thermo Fisher Scientific), whereas a ZEISS Celldiscoverer 7 (ZEISS) automated microscope was used to capture fluorescent images. Brightness and colour contrast were adjusted, and images were analysed using ImageJ software.

Flow cytometry

The proximal third of the gastrocnemius was immediately processed for flow cytometry.²² Briefly, muscles were digested in Miltenyi gentleMACS C tube (Cat# 130-093-237, Miltenyi Biotec) containing Collagenase B (1.5 U/mL, Cat# 11088831001, Sigma-Aldrich) and Dispase II (2 U/mL, Cat# 42613-33-2, Sigma-Aldrich) in Ham's F10 media (Cat# 318-050-CL, Wisent Inc) by gentleMACS Octo Dissociator (Cat# 130-096-427, Miltenyi Biotec). The resulting muscle slurry was filtered (100 μm; Cat# 22-363-549, Fisher Scientific) and then treated with Red Blood Cell Lysing Buffer (Cat# R7767, Sigma-Aldrich). Cells were incubated with FITC Rat Anti-Mouse CD45 (Cat# 561088, BD Biosciences), BV510 Rat Anti-Mouse CD31 (Cat# 563089, BD Biosciences), anti-Alpha 7 Integrin (ITGA7) 647 (Cat# 67-0010-05, AbLab) and BV711 Rat Anti-Mouse Ly-6A/E (Sca1) (Cat# 563992, BD Biosciences) in flow buffer (10% FBS, 3 mM of EDTA in 1× PBS) for 35 min. Cell viability was assessed with SYTOX Green (Cat# S34860, Invitrogen). Cell populations of interest were haematopoietic (CD31⁻/CD45⁺), endothelial (CD45⁻/CD31⁺), MuSCs (CD45⁻/ CD31⁻/ITGA7⁺) and FAPs (CD45⁻/CD31⁻/ITGA7⁻/Sca1⁺). Analysis was performed using an NxT flow cytometer and processed in FlowJo v10.8 Software (BD Life Sciences) with gates and compensation established using fluorescence minus one and single-stained controls.

NanoString nCounter assay and data analysis

Total RNA isolation from flash frozen gastrocnemius was performed using Micro Kit (Cat# 74004, Qiagen) according to

manufacturer's instructions. RNA purity and concentration were measured with a NanoDrop 2000c spectrophotometer (Thermo Fisher Scientific). Targeted transcriptomic analysis of a specific CodeSet panel of genes involved in muscle fibrosis and inflammation was performed with a NanoString nCounter Mouse Fibrosis V2 panel (Cat# 115000388, NanoString Technologies). Samples (100 ng of RNA) were prepared and analysed on the multiplexed digital nCounter® platform (NanoString Technologies) according to the manufacturer's instructions. Reporter code count (RCC) and reporter library file (RFL) were generated, and quality control, background subtraction and normalization were performed using the nSolver 4.0 software (NanoString Technologies). Normalized RCC files were analysed using ROSALIND® nCounter Data Analysis Software (https://rosalind.bio/), with a HyperScale architecture developed by OnRamp BioInformatics, Inc. A multidimensional scaling (MDS) plot was generated, and the cell-type profiling module-quantified cell populations, fold changes and P values were calculated based on the fast method (nCounter Advanced Analysis MAN-10030-03). The Benjamini-Hochberg method of estimating false discovery rates (FDRs) was used for the adjusted P value. Gene clusters for heatmaps of differentially expressed genes (DEGs) were created using the Partitioning Around Medoids (PAM) method using the fpc R library.²³ Hypergeometric distribution was performed to analyse the enrichment of pathways, Gene Ontology (GO) and other ontologies. The topGO R library²⁴ was used to determine local similarities and dependencies between GO terms. Gene set analysis (GSA) and GO terms were performed using the DEGs.

Statistical analyses

Analyses were blinded. Data are expressed as mean \pm standard error of the mean (SEM) with $P \leq 0.05$ considered significant. A three-way mixed analysis (time \times group \times treatment) of variance or a two-way mixed analysis (treatment \times group) of variance were used where appropriate followed by Sidak post hoc tests using GraphPad Prism Version 8.0.1 software (GraphPad Software).

Results

Mouse survival and tumour recurrence

Four mice, two males and one female in RET and one male in SED, perished during the intervention. Three male mice likely died due to tumour recurrence and metastases, whereas the female mice sustained an injury during RET that required sacrifice. Therefore, a total of 16 mice (SED = 9 and RET = 7)

were used for downstream analyses except for immunohistochemistry where muscles for six mice in the RET group (n = 6) and eight mice in the SED group (n = 8) were of sufficient quality to use for myonuclear and MyHC analyses.

Resistance and endurance exercise training improves endurance performance and body composition after rhabdomyosarcoma plus therapy

Mice in the RET group ran approximately 5.86 ± 0.44 km/day, which was consistent across the 8-week intervention (*Figure S1A*). RET had higher endurance performance than SED at Post-RET (*Figure 1B*, group effect P < 0.0001), with no sex difference (*Figure S1B*, P = 0.004). Absolute and relative grip strength increased at Pre-RET compared to Pre-Tx and further increased at Post-RET (*Figure S1C*,D, time effect P < 0.0001). Body weight increased between baseline and Post-RET (*Figure 1C*, time effect P < 0.0001). RET had less body fat percentage than SED at Post-RET (*Figure 1D*, group effect P = 0.0004). Lean mass increased between Pre-RET and Pre-Tx and was further increased Post-RET (*Figure 1E*, time effect P < 0.0001).

Rhabdomyosarcoma plus therapy induced muscle atrophy and fibrosis

Gastrocnemius weight was lower in RMS + Tx than CON (Figure 2A, treatment effect P < 0.05) and higher in RET than SED (Figure 2A, group effect P < 0.05). More extracellular matrix accumulated in RMS + Tx than CON (Figure 2B, treatment effect P = 0.028). Representative Masson's trichrome images are presented (Figure 2C).

Resistance and endurance exercise training induced myofibre hypertrophy and alterations in fibre-type distribution independent of rhabdomyosarcoma plus therapy

Representative MyHC images are presented (*Figure 3A*). MyHC Type I and hybrid fibres were inconsistently detected across samples and thus were excluded from final analyses. Total fibre CSA was larger in RET than SED (*Figure 3B*, group effect P = 0.0087). SED had more 2000- to 2400- μ m² fibres than RET in the CON limb (*Figure S2A*, P = 0.011) and a trend for more fibres < 400 μ m² in SED than RET in the RMS + Tx limb (*Figure S2B*, P = 0.065). Type IIA CSA was larger in RET than SED (*Figure 3C*, group effect P = 0.014). Type IIB CSA was smaller in RMS + Tx than CON (*Figure 3D*, treatment effect P = 0.006) and was larger

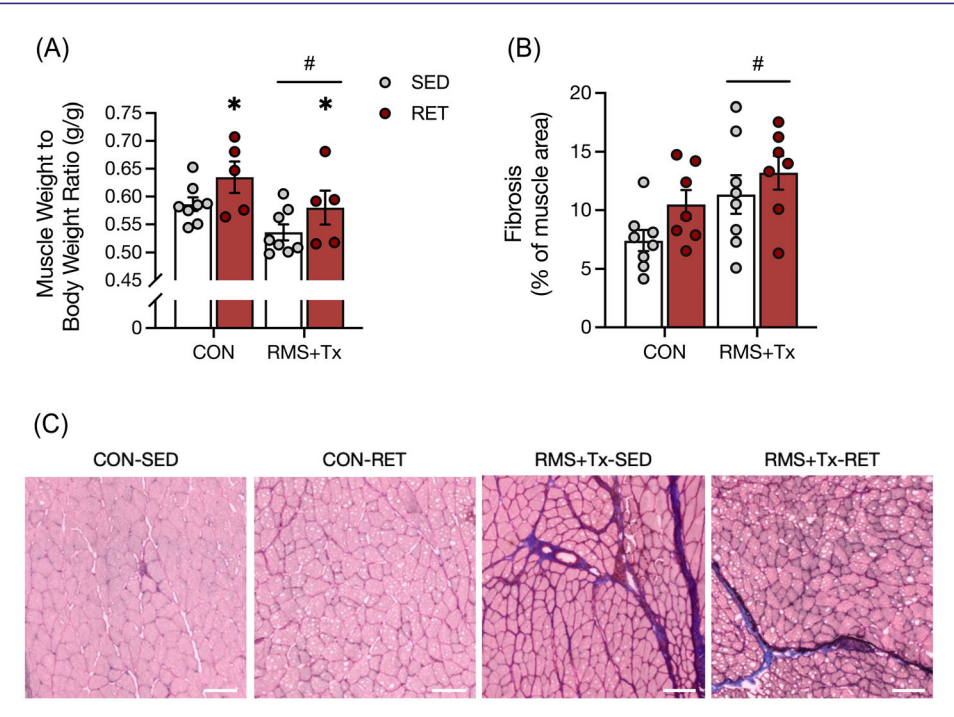


Figure 2 Rhabdomyosarcoma (RMS) plus therapy induces muscle atrophy and fibrosis. (A) Muscle weight relative to total body weight (g/g). (B) Quantification of trichrome stain for intramuscular fibrosis and collagen content as a % of total muscle area. (C) Representative images of trichrome staining for intramuscular fibrosis and collagen content. Scale = $100 \mu m$. *P < 0.05, SED versus RET. *P < 0.05, RMS + Tx versus CON. Two-way analysis of variance (ANOVA), Sidak post hoc test. $P = 1.00 \mu m$.

in RET than SED (*Figure 3D*, group effect P = 0.015). Type IIX CSA was not altered (*Figure S2C*). The proportion of Type IIA fibres was higher in RMS + Tx than CON (*Figure 3E*, treatment effect P = 0.004) and was also higher in RET than SED (*Figure 3E*, group effect P = 0.025). Fewer Type IIB fibres were observed in RMS + Tx than CON (*Figure 3F*, treatment effect P = 0.006) as well as in RET than SED (*Figure 3F*, group effect P = 0.025). No differences in Type IIX fibre proportion were observed (*Figure S2D*).

Increase in myonuclear domain with no changes in myonuclear accretion followed rhabdomyosarcoma plus therapy and resistance and endurance exercise training

Representative myonuclear and laminin staining is presented (*Figure 4A*). Total myonuclear domain was larger in CON-RET than RMS + Tx-RET (*Figure 4B*, P < 0.001). Type IIA myonuclear domain was larger in RET than SED (*Figure 4C*, group effect P = 0.001). A larger domain was observed in Type IIB fibres in CON-RET than CON-SED (P = 0.013) and RMS + Tx-RET ($P \le 0.001$) (*Figure 4D*). A trend for greater myonuclear domain size was also observed in RET than SED for Type IIX fibres (*Figure 4E*, group effect P = 0.086). No differences in nuclei per fibre were observed (*Figure S3A-D*).

Rhabdomyosarcoma plus therapy and resistance and endurance exercise training induce changes in cellular dynamic in skeletal muscle

Representative flow plots for skeletal muscle mononuclear cell populations are presented (*Figure S4A*). Total live, mononuclear cell count per muscle weight was lower in RMS + Tx than CON (*Figure S4B*, treatment effect P < 0.05). RMS + Tx had a higher number (*Figure 5A*, treatment effect P < 0.05) and proportion of CD45⁺ cells than CON (*Figure S4C*, treatment effect P < 0.05). More CD31⁺ cells in RET than SED mice were observed in the RMS + Tx limb (*Figure 5B*, P < 0.05). RET had a higher proportion of CD31⁺ cells than SED (*Figure S4D*, group effect P < 0.05). RMS + Tx had fewer α 7⁺ cells than CON (*Figure 5C*, treatment effect P < 0.05) with no difference in α 7⁺ cell proportion (*Figure S4E*). RET had more (*Figure 5D*, group effect P = 0.022) and a higher proportion (*Figure S4F*, group effect P < 0.05) of Sca1⁺ cells than SED.

Fibrotic and inflammatory transcriptome is induced by rhabdomyosarcoma plus therapy and is partially prevented by resistance and endurance exercise training

The MDS plot distinguishes CON and RMS + Tx groups independent of RET/SED condition (*Figure S5A*). CellProfiler

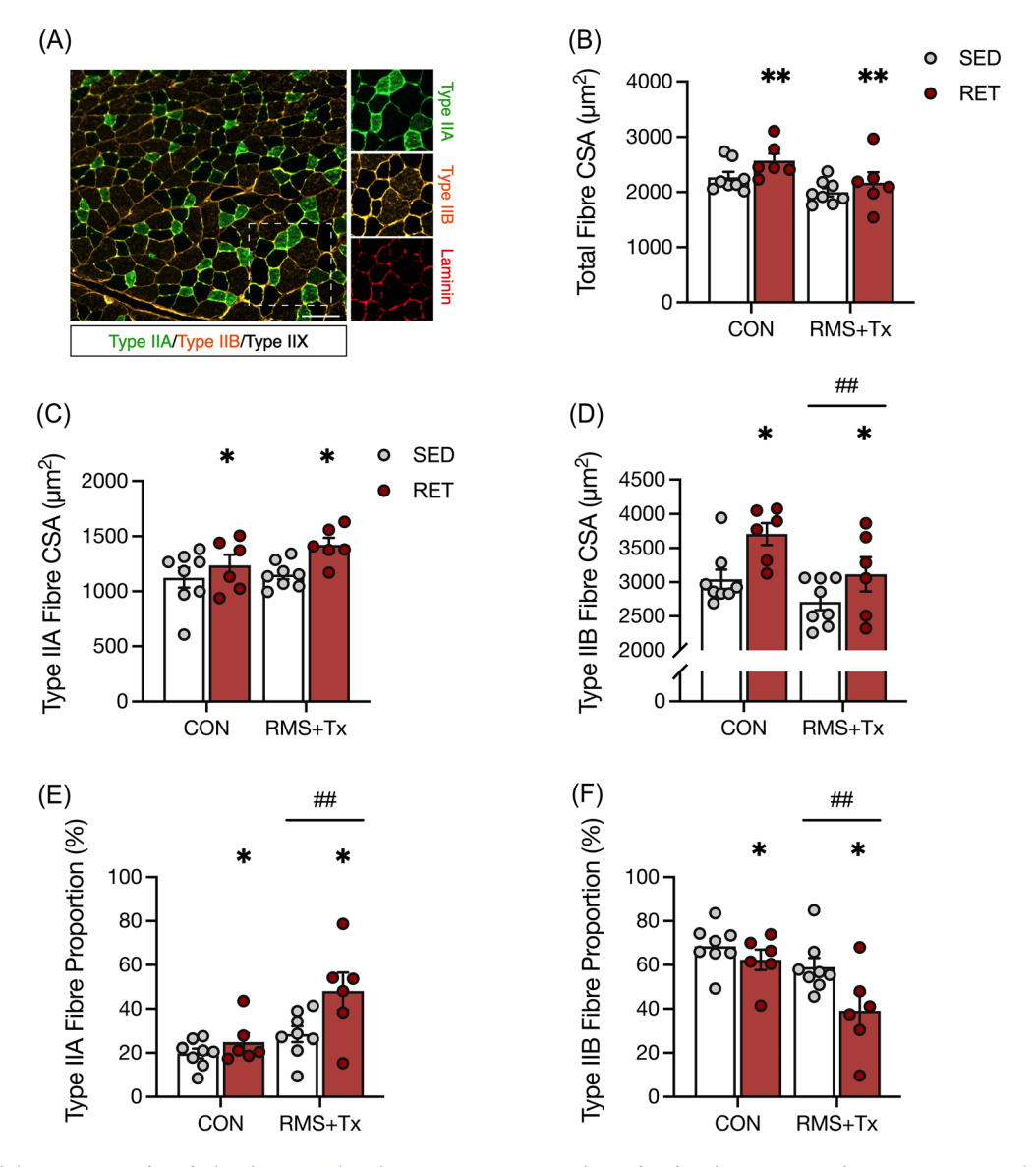
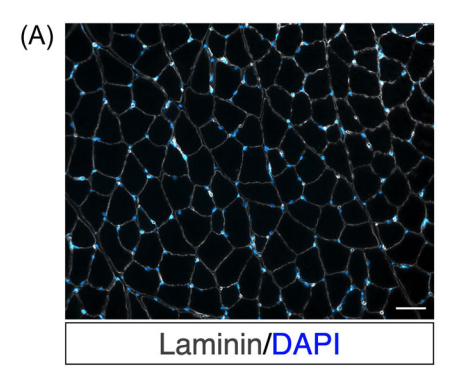


Figure 3 Rhabdomyosarcoma (RMS) plus therapy reduced Type IIB cross-sectional area (CSA) and proportion, whereas resistance and endurance exercise training (RET) enlarged myofibre CSA and induced alterations in fibre-type distribution independent of RMS plus therapy. (A) Representative image of myosin heavy chain stain immunofluorescence (Type IIA: green; Type IIB: orange; Type IIX: black; laminin: red). (B) Total fibre CSA (μ m²). (C) Type IIA fibre-specific CSA (μ m²). (E) Proportion of Type IIA fibres (% of total fibre number). (F) Proportion of Type IIB fibres (% of total fibre number). *P < 0.05 and *P < 0.01, SED versus RET group. *P < 0.01, RMS + Tx versus CON. Two-way analysis of variance (ANOVA), Sidak post hoc test. P = 6-8 per group. Scale = 100 μ m.

indicates an enrichment of mast cells, macrophages and CD45⁺ cells in RMS + Tx versus CON (*Figure S5B*). A volcano plot identifies the DEGs up-regulated (\log_2 fold change > +0.5) and down-regulated (\log_2 fold change < -0.5) between CON-RET and CON-SED is presented (*Figure 6A, P* < 0.05). Eight genes (*Cd36, Cxcr4, Gbp3, Oasl1, Tnfsf10, Mmp12* and *Angptl4*) were up-regulated and four genes were down-regulated (*Lep, Adipoq, Irf4* and *S100a4*) in the CON-RET compared with CON-SED. The Top 10 GSA revealed up-regulated genes for macrophage activation, chemokine signalling, fatty acid and cholesterol metabolism, oxidative stress and others in

CON-RET versus CON-SED (*Figure 6A*). Comparing RMS-RET to RMS-SED, three genes were up-regulated (*Dapk1*, *Tm6fs2* and *Ptger4*) and three were down-regulated (*Ccl2*, *Cd163* and *Myd88*) (*Figure 6B*). The Top 10 GSA revealed down-regulated genes for cell cycle, ECM remodelling and others with up-regulated genes for Th1 differentiation (*Figure 6B*).

A total of 117 genes were up-regulated in RMS-SED versus CON-SED (*Figure 6C*, P < 0.05). GSA revealed genes enriched for macrophage activation, interferon, chemokine signalling and others (*Figures 6C* and *S5C*). Biological process GO terms, based on the up-regulated genes, showed genes involved



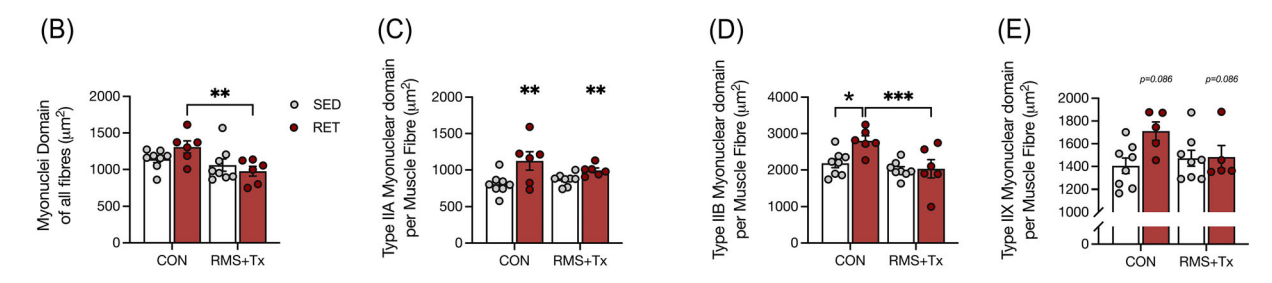


Figure 4 Resistance and endurance exercise training (RET) enlarged myonuclear domain with no changes in myonuclear accretion followed rhabdomyosarcoma (RMS) plus therapy. (A) Representation of images used for quantifying myonuclei and myonuclear domain. (B) Myonuclear domain of all fibres (μm^2). (C) Type IIA fibre-specific myonuclear domain (μm^2). (D) Type IIB fibre-specific myonuclear domain (μm^2). (E) Type IIX fibre-specific myonuclear domain (μm^2). *P < 0.05, *P < 0.01 and ***P < 0.001. Two-way analysis of variance (ANOVA), Sidak post hoc test. P = 0.01 and ***P < 0.001. Two-way analysis of variance (μm^2).

mostly in the immune response in RMS-SED versus CON-SED (*Figure 6C*, FDR, adjusted *P* value < 0.05). Conversely, 124 genes were up-regulated and 1 down-regulated (*Ppara*) in RMS-RET versus CON-RET (*Figure 6D*, P < 0.05). These genes were enriched for complement activation, collagen biosynthesis and modification, ECM degradation, and cytokine and chemokine signalling among others in RMS-RET (*Figures 6D* and *S5D*). Biological process GO terms showed genes involved in the immune response and collagen organization among others (*Figure 6D*, FDR, adjusted *P* value < 0.05). Higher Mmp-2 (P = 0.005) and Col3a1 (P = 0.028) gene expression in RMS-RET than CON-RET was confirmed by qPCR (*Figure S5E*). Higher active MMP-2 (P = 0.0068) and CCR2

(P = 0.018) protein in RMS-RET than CON-RET was confirmed by Western Blot (Figure 6E,F).

Discussion

The overall objective of this study was to determine the extent to which RET can prevent the negative long-term consequences of RMS plus therapy in skeletal muscle. Our main findings were that RET improved body composition and enhanced endurance performance, induced Type II myofibre hypertrophy, increased the number of several mononuclear

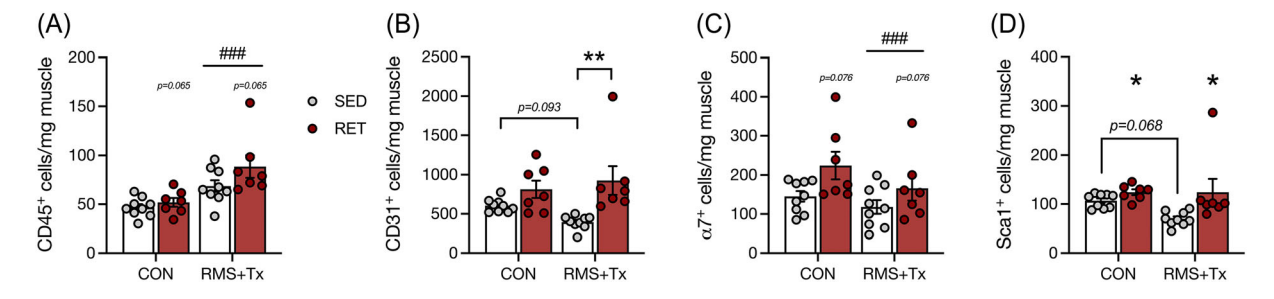


Figure 5 Rhabdomyosarcoma (RMS) plus therapy and resistance and endurance exercise training (RET) alter cellular dynamic in skeletal muscle. (A) CD45⁺ cells per mg of muscle. (B) CD31⁺ cells per mg of muscle. (C) α 7⁺ cells per mg of muscle. (D) Sca1⁺ cells per mg of muscle. * $^*P < 0.05$ and * $^*P < 0.01$, SED versus RET. * $^{###}P < 0.001$, RMS + Tx versus CON. Two-way analysis of variance (ANOVA), Sidak post hoc test. $^*P = ^*P = ^*P = ^*P$ per group.

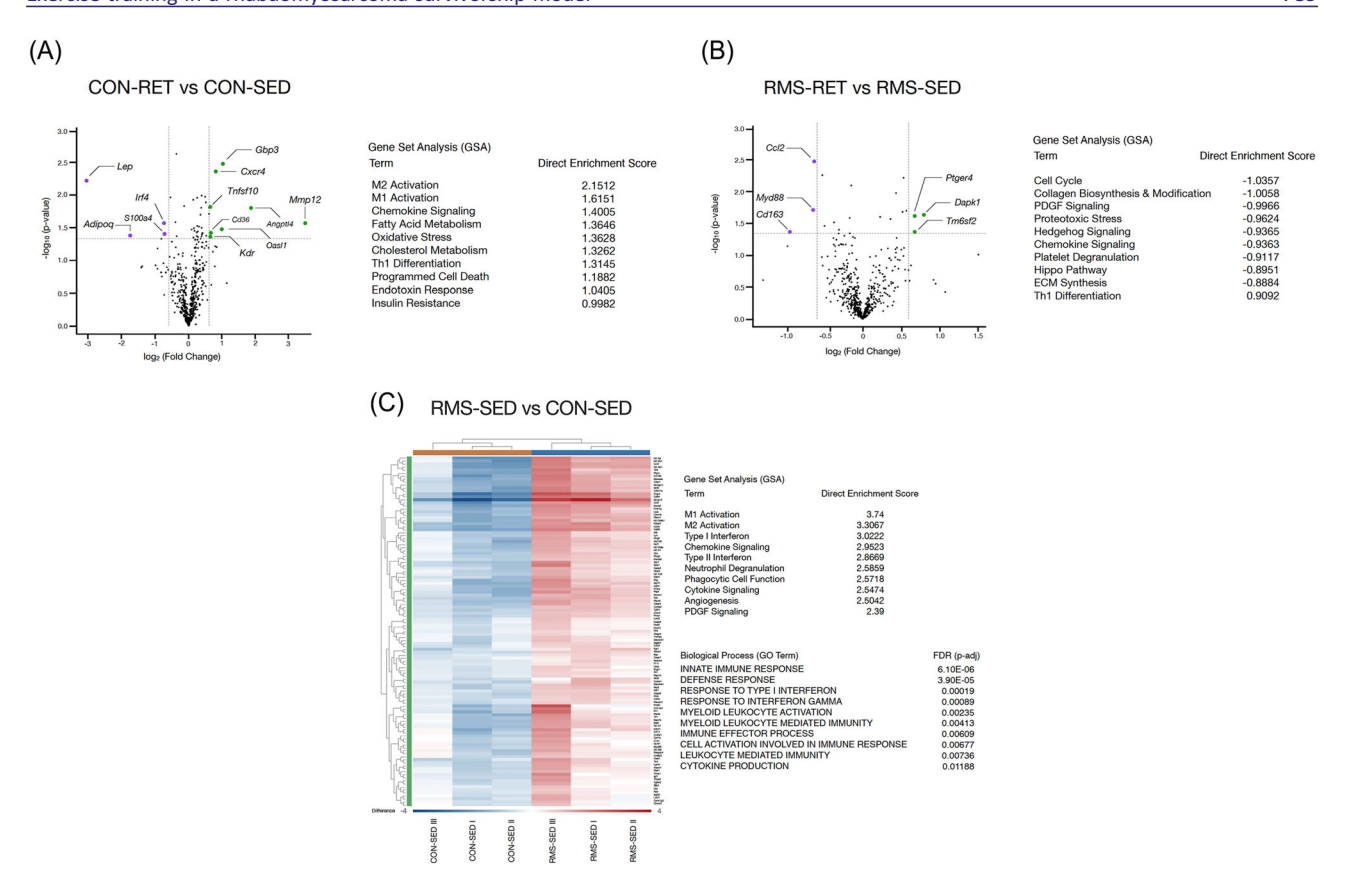
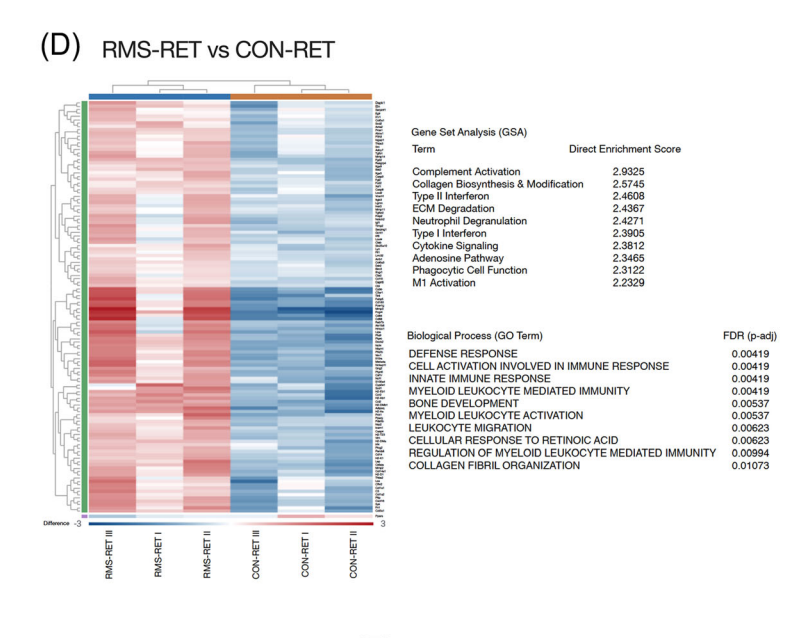


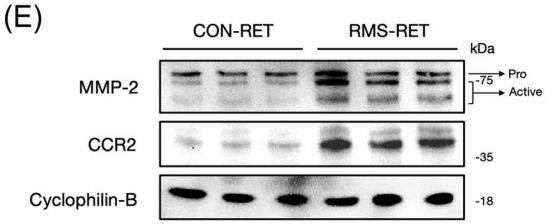
Figure 6 Fibrotic and inflammatory signature is induced by rhabdomyosarcoma (RMS) plus therapy and is partially reduced by resistance and endurance exercise training (RET) in skeletal muscle. (A) Volcano plot of \log_2 -transformed fold change and $-\log_{10}$ -transformed P values showing up-regulated (in green) and down-regulated (in purple) genes in CON-RET versus CON-SED and the Top 10 direct enrichment score from the gene set analysis (GSA). (B) Volcano plot of \log_2 -transformed fold change and $-\log_{10}$ -transformed P values showing up-regulated (in green) and down-regulated (in purple) genes in RMS-RET versus RMS-SED and the Top 10 direct enrichment score from the gene set analysis (GSA). (C) Heatmap of differentially expressed genes (DEGs) in RMS-SED versus CON-SED, Top 10 (GSA) in RMS-SED versus CON-SED and Top 10 biological process Gene Ontology (GO) terms (false discovery rate [FDR], adjusted P value) in RMS-SED versus CON-SED. (D) Heatmap of DEGs in RMS-RET versus CON-RET, Top 10 GSA in RMS-RET versus CON-RET and Top 10 biological process GO terms (FDR, adjusted P value) in RMS-RET versus CON-RET. (E) Representative western blot image of MMP-2, CCR2 and cyclophilin B protein expression. (F) Fold change of pro-MMP-2, active MMP-2 and CCR2 protein expression, normalized by cyclophilin B. *P < 0.05 and *P < 0.01. P = 3 per condition.

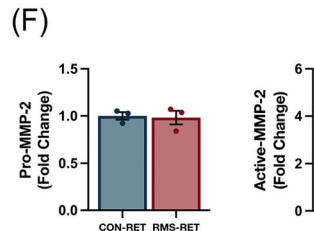
cells involved in supporting muscle maintenance and partially prevented the inflammatory/fibrotic gene signature induced by RMS plus therapy. These results suggest that RET-based interventions reduce the negative long-term effects of RMS plus therapy, in part by improving the skeletal muscle micro-environment.

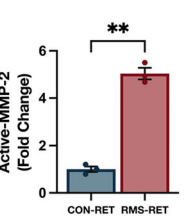
Excess adiposity and impaired physical performance leading to reduced participation in physical activity is commonly reported among cancer survivors. We showed that RET leads to improved body composition and exercise performance. Adiposity did not increase in RET mice following RMS plus therapy, whereas SED mice experienced an almost two-fold increase in total body fat percentage, which aligns with previous work from our group. Conversely, RET did not alter the increases in body weight and lean mass observed over the course of the study, likely due to the period of juvenile growth and development and the effects of RET on muscle

hypertrophy not being detected by less sensitive whole-body measures. The increases in grip strength in our study were likely due to the period of growth and development of the mice. However, a limitation of our study is that we were not able to assess a direct strength measure of the gastrocnemius due to the data collection across multiple time points in the same mice. Adherence to exercise programmes in cancer survivors is often a barrier to their efficacy.²⁵ Mice in the RET group effectively sustained the voluntary exercise protocol for 8 weeks with increasing resistance. Daily distance travelled in our RMS plus therapy model was similar to previous work in aged mice. 26,27 Thus, our preclinical juvenile RMS plus therapy model appears to show a similar premature ageing response that has been described in human cancer survivor.²⁸ Further, the RET protocol induced a 200% increase in endurance performance following RMS plus therapy. These results agree with previous literature from our group that de-









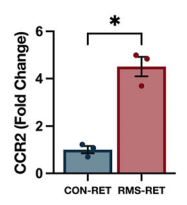


Figure 6 Continued

scribe increases in muscular performance in mouse models of cancer survivorship. ¹⁹ In conclusion, these findings indicate that sustained adherence to RET leads to improvements in whole-body composition and enhanced endurance performance in a model of RMS plus therapy.

Previous work has shown that RET causes myofibre hypertrophy and can lead to fibre-type adaptations that favour a more oxidative profile in healthy and aged mice. 16,29 We confirm and extend these findings by showing that RET induces hypertrophy in both Type IIA and Type IIB myofibres and supports a shift from Type IIB to Type IIA fibres in a model of juvenile cancer survivorship. Interestingly, RMS + Tx only resulted in significantly smaller fibres in Type IIB. Based on these results, RET induced hypertrophy in total fibres and in Type IIA fibres as evidenced by larger CSA with RET and no change in CSA in RMS + Tx. Conversely, in Type IIB fibres, RET likely prevented atrophy given the smaller CSA in RMS + Tx and larger CSA in RET. As such, the effects of RET and RMS + Tx in this model seem fibre-type dependent. Interestingly, our targeted gene expression analysis revealed a significant difference in genes involved in the mTOR signalling pathway and a significant down-regulation in genes involved in the TGF-β pathway, which support a combined pro-hypertrophic and anti-atrophic effect of RET. The results obtained in the present study largely align with and extend findings from the Deminice lab, which used a model of cachexia but not cancer survivorship, a different resistance training model that lacked an endurance component, a different species³⁰/strain of mice,³¹ and did not conduct fibre type-specific analyses.^{30,31} Taken together, these data support the concept that a hybrid resistance—endurance exercise programme can have dual effects of enhancing endurance and inducing hypertrophy.

Juvenile muscle growth requires functioning MuSCs providing for the addition of new myonuclei to myofibres.⁸ Previous work using the same RMS plus therapy model showed that treatment-induced depletion of MuSCs underlies impaired muscle development.⁵ Further, RET has been shown to elevate MuSC content, 16 whereas MuSC ablation impairs muscle adaptation to RET.²⁹ Our results support these findings showing that MuSCs were depleted by RMS plus therapy, with a trend for more MuSCs in RET. Intriguingly, no changes in nuclei per fibre were found between groups; however, a significant increase in the myonuclear domain was apparent in Type IIA fibres in RET compared to SED, as well as for Type IIX fibres in the control limb of RET compared to SED. This is in contrast to previous work that reports increased number of myonuclei per fibre in RET versus SED groups in both young and aged mice. 16,29 These data suggest that the muscle hypertrophy seen in RET mice following RMS plus therapy is driven primarily by protein synthesis, independent of myonuclear accretion. Indeed, our transcriptional profiling indicated a slight down-regulation of the mechano-sensitive Hippo pathway, which would be expected to activate muscle protein synthesis.³² Further, these data suggest that the MuSC pool is still defective in RMS plus therapy even after an exercise intervention.

MuSCs are regulated by their local micro-environment, which includes several cell types, including FAPs. In line with previous work, 6 RMS plus therapy did not result in FAP depletion; however, we did observe a trend for fewer FAPs in RMS + Tx-SED versus CON-SED. Conversely, we observed significantly more FAPs following RET in both CON and RMS plus therapy, which aligns with previous preclinical models of endurance exercise 15,20,33 and resistance training studies in humans.³⁴ Further, we detected more fibrosis in the RMS plus therapy condition, 15 which aligns with our transcriptional analysis that showed an enrichment in genes involved in platelet-derived growth factor (PDGF) signalling in RMS + Tx-SED compared to CON-SED. PDGF signalling is involved in sarcoma formation³⁵ and promotes fibrosis by inducing FAP differentiation into myofibroblast leading to excess ECM accumulation. 36,37 Thus, the trend for a reduction in FAPs by RMS plus therapy could be due to their myofibroblast differentiation, which contributed to the observed ECM accumulation in RMS + Tx. Although RET had no effect on muscle fibrosis, which was similar to our previous work with endurance exercise following radiation exposure, 15 genes involved in PDGF and Hedgehog signalling, two pro-fibrotic pathways, 37,38 were down-regulated in the RMS + Tx-RET compared to RMS + Tx-SED, suggesting RET as a potential exercise intervention to decrease the fibrogenic potential of FAPs. Hypertrophic stimuli induce ECM remodelling by stimulating pathways involved in ECM degradation and synthesis, which facilitates ECM reorganization and promotes myofibre growth.³⁹ Our transcriptomic data indicate that ECM reorganization is ongoing in RET facilitated by diverse matrix metalloproteinases (Mmp14, Mmp3, Mmp2, etc.) and with collagen biosynthesis and modification and collagen degradation pathways both enriched in RMS + Tx-RET versus RMS + Tx-SED. Consistent with our results, Peck et al. showed that mechanical overload increased Mmp14 gene expression, which was correlated with more macrophages and skeletal muscle adaptation in humans following resistance exercise training.40 Similarly, our study showed that MMP-2 protein expression was higher in RMS-RET than CON-RET, aligning with the increase in macrophages in RMS + Tx versus CON observed in our transcriptomic data. Similarly, CCR2 was up-regulated in RMS + Tx. which is also associated with muscle inflammation and impaired regeneration. S1 Thus, MMP-2 and CCR2 are potential targets to improve the effects of RMS plus therapy on skeletal muscle.

Endothelial cells are another component of the MuSC niche, and the perivascular location of FAPs and MuSCs suggests the strong communication with ECs. S2 Endothelial cell

loss is radiation dose dependent and progressive and contributes to myofibroblast activation and muscle fibrosis. ¹⁰ When FAPs are genetically depleted, disrupting FAP–EC crosstalk results in impaired skeletal muscle revascularization and fibrosis following hindlimb ischaemia. ⁵² We detected a trend for fewer ECs in the RMS plus therapy model, which mirrors our FAP findings. Also, similar to our FAP results, RET increased ECs, suggesting pro-angiogenic features of RET that could improve skeletal muscle perfusion and facilitate crosstalk between ECs and FAPs.

Previous work suggested that long-term up-regulation of inflammatory genes was involved in muscle degradation using the same RMS plus therapy model. Similarly, we found an increase in cell abundance score of macrophages and haematopoietic cells, supported by flow cytometry analysis that showed higher quantity of haematopoietic cells following RMS plus therapy. Several genes involved in the immune and inflammatory response were also up-regulated in RMS + Tx in our transcriptional analyses. Immune cells, especially macrophages, are a key component of muscle regeneration and adaptation but also in chronic inflammatory conditions. S3 In our study, RMS plus therapy increased genes related to M1 (generally pro-inflammatory) and M2 (generally anti-inflammatory) macrophage activation (i.e., Ccr2, Ccl2 and Cxcr4) as well as genes involved in interferon signalling (i.e., H2-Aa and Isg15a), and this heightened and prolonged inflammatory response aligns with previous work.⁶ Excitingly, RET down-regulated Ccl2, Myd88 and Cd163 in RMS + Tx, which are all genes involved in pro-inflammatory signalling. Although RET in the CON limb showed higher M1- and M2-related genes than SED, this aligns with a previous finding that shows the necessity of macrophage recruitment to induce muscle hypertrophy following mechanical overload. S4 Thus, RET may inhibit the negative long-term late effects of RMS plus therapy by reducing inflammation.

Together, our results show that RET improves endurance performance and body composition and induces skeletal muscle hypertrophy in a model of juvenile RMS plus therapy. These effects were mediated by positive changes in cellular dynamics, including increases in ECs and FAPs and a partial reversal of the inflammatory and fibrotic gene signature. As such, our study indicates that skeletal muscles can adapt to RET following RMS plus therapy and suggests that increased protein synthesis and improvements in the muscle micro-environment may be the primary mechanisms responsible.

Acknowledgements

We acknowledge the Mackall Lab at Stanford for generously providing the M3-9-M cells. We also acknowledge Katey Rayner and Michele Geoffrion from the Ottawa Heart Insti-

tute, and the Department of Biochemistry, Microbiology and Immunology, Faculty of Medicine, at the University of Ottawa, for their assistance with the NanoString assay. We acknowledge the services of The Behavioural Core Facility, The Louise Pelletier Histology Core Facility and the Pre-clinical Imaging Core Facility at the University of Ottawa. We acknowledge Isabel Rodriguez for her assistance with the myonuclear domain analysis. Finally, we also acknowledge the important published work that could not be cited due to limitations on word count and references. This manuscript complies with the ethical guidelines for authorship and publishing in the Journal of Cachexia, Sarcopenia and Muscle. SS

Funding

This work was supported by the Natural Sciences and Engineering Research Council of Canada (NSERC), The Canadian Foundation for Innovation (CFI), discretional funds awarded

to the De Lisio Lab and the Ontario Early Researcher Award (M. D. L.). N. C. is supported by the Chilean National Agency for Research and Development (Agencia Nacional de Investigación y Desarrollo [ANID]) and the uOttawa/CHEO Research Institute's Doctoral Fellowship for Advancement of Biological Perspectives for Exercise Interventions Across the Lifespan. O. S. is supported by the Ontario Graduate Scholarship (OGS).

Conflict of interest

The authors declare no conflicts of interest.

Online supplementary material

Additional supporting information may be found online in the Supporting Information section at the end of the article.

References

- Amer KM, Thomson JE, Congiusta D, Dobitsch A, Chaudhry A, Li M, et al. Epidemiology, incidence, and survival of rhabdomyosarcoma subtypes: SEER and ICES database analysis. J Orthop Res 2019;37:2226–2230.
- Paulino AC. Late effects of radiotherapy for pediatric extremity sarcomas. Int J Radiat Oncol Biol Phys 2004;60:265–274.
- Stubblefield MD. Radiation fibrosis syndrome: neuromuscular and musculoskeletal complications in cancer survivors. PM R 2011;3:1041–1054.
- Bachman JF, Blanc RS, Paris ND, Kallenbach JG, Johnston CJ, Hernady E, et al. Radiation-induced damage to prepubertal Pax7+ skeletal muscle stem cells drives lifelong deficits in myofiber size and nuclear number. iScience 2020;23:101760.
- Paris ND, Kallenbach JG, Bachman JF, Blanc RS, Johnston CJ, Hernady E, et al. Chemoradiation impairs myofiber hypertrophic growth in a pediatric tumor model. *Sci Rep* 2020;**10**:19501.
- Kallenbach JG, Bachman JF, Paris ND, Blanc RS, O'Connor T, Furati E, et al. Muscle-specific functional deficits and lifelong fibrosis in response to paediatric radiotherapy and tumour elimination. J Cachexia Sarcopenia Muscle 2022;13:296–310.
- Mauro A. Satellite cell of skeletal muscle fibers.
 J Biophys Biochem Cytol 1961;9:493–495.
- 8. 9pt?>Bachman JF, Klose A, Liu W, Paris ND, Blanc RS, Schmalz M, et al. Prepubertal skeletal muscle growth requires Pax7-expressing satellite cell-derived myonuclear contribution. *Development* 2018;145:dev167197.

- Mashinchian O, Pisconti A, Le Moal E, Bentzinger CF. The muscle stem cell niche in health and disease. Curr Top Dev Biol 2018;126:23–65.
- Williams JP, Calvi L, Chakkalakal JV, Finkelstein JN, O'Banion MK, Puzas E. Addressing the symptoms or fixing the problem? Developing countermeasures against normal tissue radiation injury. Radiat Res 2016;186:1–16.
- Patsalos A, Pap A, Varga T, Trencsenyi G, Contreras GA, Garai I, et al. In situ macrophage phenotypic transition is affected by altered cellular composition prior to acute sterile muscle injury. *J Physiol* 2017;595: 5815–5842.
- Campbell KL, Winters-Stone KM, Wiskemann J, May AM, Schwartz AL, Courneya KS, et al. Exercise guidelines for cancer survivors: consensus statement from international multidisciplinary roundtable. *Med Sci Sports Exerc* 2019;51:2375–2390.
- O'Connor TN, Kallenbach JG, Orciuoli HM, Paris ND, Bachman JF, Johnston CJ, et al. Endurance exercise attenuates juvenile irradiation-induced skeletal muscle functional decline and mitochondrial stress. Skelet Muscle 2022;12:8.
- De Lisio M, Kaczor JJ, Phan N, Tarnopolsky MA, Boreham DR, Parise G. Exercise training enhances the skeletal muscle response to radiation-induced oxidative stress. *Muscle Nerve* 2011;43:58–64.
- D'Souza D, Roubos S, Larkin J, Lloyd J, Emmons R, Chen H, et al. The late effects of radiation therapy on skeletal muscle morphology and progenitor cell content

- are influenced by diet-induced obesity and exercise training in male mice. *Sci Rep* 2019;**9**:6691.
- Dungan CM, Murach KA, Frick KK, Jones SR, Crow SE, Englund DA, et al. Elevated myonuclear density during skeletal muscle hypertrophy in response to training is reversed during detraining. Am J Physiol Cell Physiol 2019;316:C649–C654.
- Meadors JL, Cui Y, Chen Q-R, Song YK, Khan J, Merlino G, et al. Murine rhabdomyosarcoma is immunogenic and responsive to T-cell-based immunotherapy. *Pediatr Blood* Cancer 2011:57:921–929.
- Emmons R, Ngu M, Xu G, Hernández-Saavedra D, Chen H, de Lisio M. Effects of obesity and exercise on bone marrow progenitor cells after radiation. *Med Sci Sports Exerc* 2019;51:1126–1136.
- Farber E, Kwiecien JM, Bojic D, Ngu M, Akohene-Mensah P, Vanhie JJ, et al. Exercise improves cancer-free survival and health span in a model of radiation-induced cancer. Med Sci Sports Exerc 2021:53:2254–2263.
- Roubos S, D'Souza D, Hernández-Saavedra D, Xu G, Collao N, Emmons R, et al. Weight loss with exercise improves muscle architecture and progenitor cell populations compared with weight loss alone in mice with preneoplastic colorectal lesions. Appl Physiol Nutr Metab 2021;46:837–845.
- Dyar KA, Ciciliot S, Wright LE, Biensø RS, Tagliazucchi GM, Patel VR, et al. Muscle insulin sensitivity and glucose metabolism are controlled by the intrinsic muscle clock. *Mol Metab* 2014;3:29–41.

- Feige P, Rudnicki MA. Isolation of satellite cells and transplantation into mice for lineage tracing in muscle. *Nat Protoc* 2020;15: 1082–1097.
- 23. Hennig C. CRAN—package fpc. https://cran.rproject.org/web/packages/fpc/index.html
- Alexa A, Rahnenfuhrer J. topGO: enrichment analysis for Gene Ontology. R package version 1.38.1. 2019.
- Courneya KS, Friedenreich CM, Quinney HA, Fields ALA, Jones LW, Vallance JKH, et al. A longitudinal study of exercise barriers in colorectal cancer survivors participating in a randomized controlled trial. *Ann Behav Med* 2005;29:147–153.
- Englund DA, Murach KA, Dungan CM, Figueiredo VC, Vechetti IJ, Dupont-Versteegden EE, et al. Depletion of resident muscle stem cells negatively impacts running volume, physical function, and muscle fiber hypertrophy in response to lifelong physical activity. Am J Physiol Cell Physiol 2020;318: C1178–C1188.
- Dungan CM, Brightwell CR, Wen Y, Zdunek CJ, Latham CM, Thomas NT, et al. Muscle-specific cellular and molecular adaptations to late-life voluntary concurrent exercise. Function (Oxf) 2022;3:zqac027.
- van Brussel M, Takken T, Lucia A, van der Net J, Helders PJM. Is physical fitness decreased in survivors of childhood leuke-

- mia? A systematic review. *Leukemia* 2005; **19**:13–17.
- Englund DA, Figueiredo VC, Dungan CM, Murach KA, Peck BD, Petrosino JM, et al. Satellite cell depletion disrupts transcriptional coordination and muscle adaptation to exercise. Function 2021:2.
- Padilha CS, Cella PS, Chimin P, Voltarelli FA, Marinello PC, Testa MTDJ, et al. Resistance training's ability to prevent cancer-induced muscle atrophy extends anabolic stimulus. Med Sci Sports Exerc 2021;53: 1572–1582.
- de Jesus Testa MT, Cella PS, Marinello PC, Frajacomo FTT, de Souza Padilha C, Perandini PC, et al. Resistance training attenuates activation of STAT3 and muscle atrophy in tumor-bearing mice. Front Oncol 2022;12:880787.
- 32. Watt Kl, Turner BJ, Hagg A, Zhang X, Davey JR, Qian H, et al. The Hippo pathway effector YAP is a critical regulator of skeletal muscle fibre size. *Nat Commun* 2015;**6**:6048.
- Saito Y, Chikenji TS, Matsumura T, Nakano M, Fujimiya M. Exercise enhances skeletal muscle regeneration by promoting senescence in fibro-adipogenic progenitors. *Nat Commun* 2020;11:889.
- Farup J, de Lisio M, Rahbek SK, Bjerre J, Vendelbo MH, Boppart MD, et al. Pericyte response to contraction mode-specific resistance

- exercise training in human skeletal muscle. *J Appl Physiol* (1985) 2015;**119**:1053–1063.
- 35. Heldin C-H. Targeting the PDGF signaling pathway in tumor treatment. *Cell Commun Signal* 2013;**11**:97.
- Kendall RT, Feghali-Bostwick CA. Fibroblasts in fibrosis: novel roles and mediators. Front Pharmacol 2014;5:123.
- Farup J, Just J, de Paoli F, Lin L, Jensen JB, Billeskov T, et al. Human skeletal muscle CD90⁺ fibro-adipogenic progenitors are associated with muscle degeneration in type 2 diabetic patients. *Cell Metab* 2021;33: 2201–2214.e11.
- Horn A, Palumbo K, Cordazzo C, Dees C, Akhmetshina A, Tomcik M, et al. Hedgehog signaling controls fibroblast activation and tissue fibrosis in systemic sclerosis. Arthritis Rheum 2012;64:2724–2733.
- Brightwell CR, Latham CM, Thomas NT, Keeble AR, Murach KA, Fry CS. A glitch in the matrix: the pivotal role for extracellular matrix remodeling during muscle hypertrophy. Am J Physiol Cell Physiol 2022;323: C763-C771.
- Peck BD, Murach KA, Walton RG, Simmons AJ, Long DE, Kosmac K, et al. A muscle cell-macrophage axis involving matrix metalloproteinase 14 facilitates extracellular matrix remodeling with mechanical loading. FASEB J 2022;36:e22155.